

Towards self-replicating materials of DNA-functionalized colloids^{†‡}

Mirjam E. Leunissen,^{*a} Rémi Dreyfus,^a Roujie Sha,^b Tong Wang,^b Nadrian C. Seeman,^b David J. Pine^a and Paul M. Chaikin^a

Received 8th October 2008, Accepted 3rd February 2009

First published as an Advance Article on the web 10th March 2009

DOI: 10.1039/b817679e

We report the first results of ongoing research that involves the creation of a new class of non-biological materials designed to self-replicate and, as a result, to grow exponentially. We propose a system design that exploits the strong specificity and thermal reversibility of the interactions between colloidal particles functionalized with complementary single-stranded DNA ‘sticky ends’. Here, we experimentally test the fundamentals of the different steps that constitute the self-replication scheme. First of all, we quantitatively study the equilibrium and kinetic aspects of the aggregation–dissociation behavior of the particles. We find that the dissociation transition is very sharp ($\sim 1\text{ }^{\circ}\text{C}$) and that it occurs at unexpectedly low temperatures, with the dissociation temperature shifting further down when the fraction of sticky ends becomes smaller. The sharpness of the transition and its sensitivity to the sticky end fraction are important control parameters in our self-replication scheme. We further find that for our present purposes it is best to use a DNA construct with a double-stranded backbone, as this largely prevents unwanted hybridization events, such as secondary structure formation. The latter is seen to lead to peculiar aggregation kinetics, due to a competition between inter- and intra-particle hybridization. Finally, we show how one can obtain dual recognition at different temperatures by functionalizing a single particle species with two distinct DNA sequences and we demonstrate the formation of permanent bonds, using the chemical intercalator psoralen and long-wavelength UV exposure.

Introduction

Looking at nature, it is evident that microscopic entities have the ability to self-replicate and to self-assemble into functional macroscopic structures. It therefore is rather surprising that artificial structures that can repeatedly copy themselves have largely remained a dream so far (note, however, the ‘molecular’ reproduction in ref. 1 and 2), in spite of the enormous potential for applications. This potential mainly lies in the exponential growth that is associated with self-replication. Exponential growth stands in sharp contrast to conventional materials production, where doubling the amount of product requires twice the production time. At present, this linear scaling poses a major stumbling block for the fabrication of useful quantities of microscopic building blocks with a sophisticated architecture, which are needed for the next stages of micro- and nanotechnology. Here, we present the first results of ongoing research that is aimed at the construction of a non-biological self-replicating system that can provide an effective manufacturing method for

such components as well as larger-scale complex functional materials. In addition, once realized, this new class of soft condensed matter systems will help us to unravel the general mechanisms by which self-replication and self-assembly work.

In broad lines, the approach to creating self-replicating materials proposed by us and illustrated in Fig. 1a, is to link a number of particles together to form the desired microscopic unit and to submerge this ‘seed’ in a bath of the individual particles that selectively interact with each other. Replication is then initiated by cyclic variations in the physical and chemical environment. Because both the seed and its copies act as templates for further replication, the number of copies should double every cycle. Although the same design principles should be applicable to materials with nanometre-sized building blocks, we use suspensions of micrometre-sized colloids for our initial explorations, because these can be readily imaged with conventional light microscopy. Together with the relatively slow particle dynamics (seconds–minutes time scales), this will allow us to follow every step of the self-replication process in great detail.³ Moreover, colloids offer the possibility of producing devices directly, such as sensors and actuators, on a mesoscopic scale (see for example ref. 4).

Active self-replication is closely related to conventional self-assembly. In both cases, a large number of components must spontaneously arrange themselves into a well-defined structure. At present, the complexity of self-assembled colloidal crystals is still very limited: ordered structures with more than two distinct components are rare. In recent years, functionalization with single-stranded complementary DNA sequences (‘sticky ends’, Fig. 2) has appeared as a prime candidate to guide particles to

^aCenter for Soft Matter Research, Physics Department, New York University, 4 Washington Place, New York, NY 10003, USA. E-mail: m.e.leunissen@nyu.edu

^bChemistry Department, New York University, 100 Washington Square East, NY 10003, USA

† This paper is part of a *Soft Matter* issue highlighting the work of emerging investigators in the soft matter field.

‡ Electronic supplementary information (ESI) available: Permanent ‘AAAAAA’ seeds were immersed in a bath of A’ singlets and at the start of the movie the temperature was decreased to 42 °C, which is below the transverse A–A’ melting temperature. The movie was taken over ~6 min. See DOI: 10.1039/b817679e

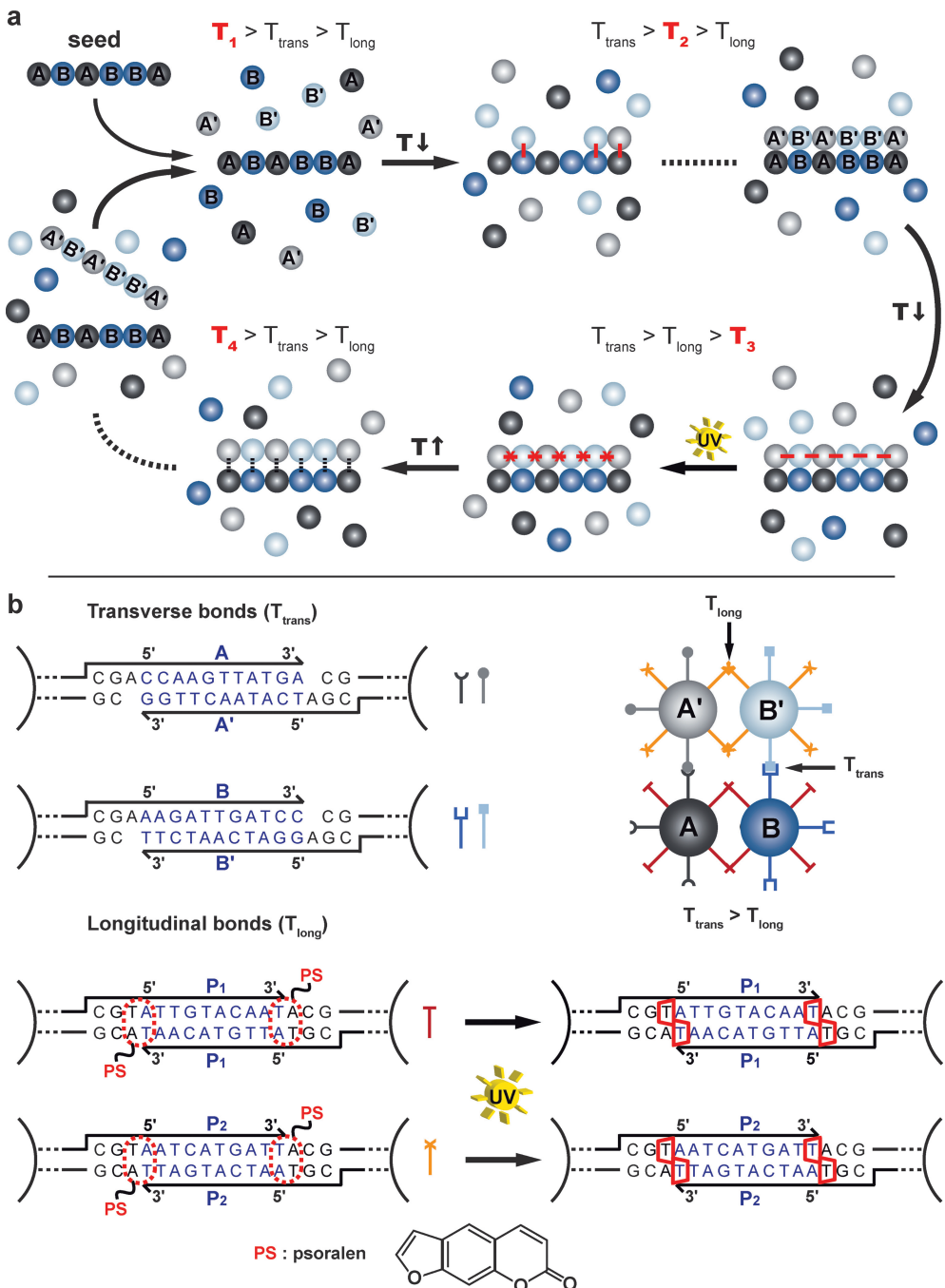


Fig. 1 The proposed DNA-mediated colloidal self-replication scheme. **a** At the start of the self-replication process we assemble a single seed structure of permanently linked A and B particles, which we introduce into a bath of free A , B , and complementary A' and B' particles, at a temperature T_1 that is higher than the melting temperature of any of the complementary pairs in the system (see also panel b). Self-replication then occurs by cycling the temperature and UV exposure, for each step we have indicated the relevant newly formed bonds in red. First, we decrease the temperature (T_2) below the melting temperature of the ‘transverse’ A - A' and B - B' bonds (T_{trans}) and let the complementary daughter chain assemble on the seed. Then, we lower the temperature further (T_3) so that the particles in the daughter chain are bound together by ‘longitudinal’ $P1$ (or $P2$) bonds (melting temperature T_{long}). We make these psoralen-functionalized longitudinal bonds permanent by UV exposure (still at T_3). Finally, we release the daughter chain from the seed by raising the temperature above the melting temperature of any of the complementary pairs in the system again (T_4), so that the non-permanent transverse bonds dehybridize. In the next cycle, both the original seed (of A and B particles) and the copy (of A' and B' particles) will function as a template. Thus, the number of copies doubles every cycle. **b** Each particle type in the self-replication scheme (A , A' , B and B') carries two different kinds of sticky ends in the following combinations (top right schematic): A - $P1$, A' - $P2$, B - $P1$, B' - $P2$ (note that in reality a particle carries thousands of sticky ends of each kind and that the DNA and particle sizes are not drawn to scale here, see also Fig. 2). The A/A' and B/B' sequences form ‘normal’ complementary pairs and constitute the transverse bonds, with melting temperature T_{trans} . On the left of the figure we show the sticky end in blue, together with the last couple of base pairs of the long double-stranded backbone in black (see also Fig. 2). The $P1$ and $P2$ sequences are self-complementary palindromic sequences and form the longitudinal bonds with melting temperature T_{long} . The backbone of the $P1$ and $P2$ constructs is functionalized with an aromatic psoralen group (PS), attached to the last base pair via a short carbon linker. This group intercalates in the two double stranded 5'-TA-3' stretches that form upon hybridization and forms a permanent cross-link between the thymine residues when excited by UV radiation.

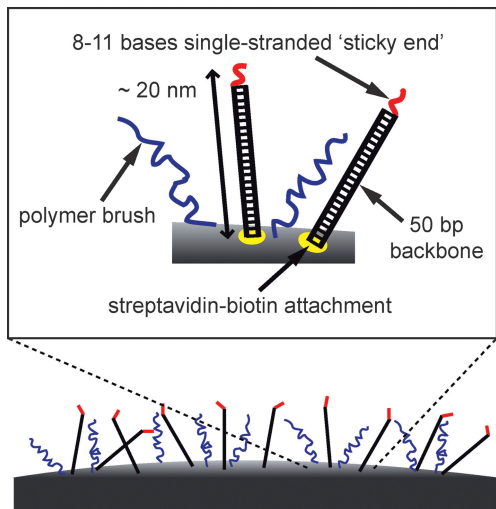


Fig. 2 The DNA-functionalized particle surface. A schematic representation of the experimental system, consisting of $1.05\text{ }\mu\text{m}$ diameter streptavidin-coated polystyrene beads, covered with short ($\sim 20\text{ nm}$), biotin-functionalized DNA. The curvature of the bead and the length of the DNA constructs are drawn to scale. The DNA constructs that we use for our self-replication scheme consist of a double-stranded ‘backbone’ (in black) with a short single-stranded sequence at its 3’ terminus, which constitutes the actual ‘sticky end’ (in red). Due to the large persistence length of double-stranded DNA ($l_p \approx 45\text{--}50\text{ nm}$),¹⁷ the backbone essentially behaves like a rigid rod. The sterically stabilizing polymer brush inhibits non-specific binding of the particles and thus promotes reversibility of the DNA-mediated binding.²⁰

their designated neighbors. Such DNA coatings form highly specific thermo-reversible linkages, whose strength and range can be finely tuned. These properties exactly meet the requirements of our self-replication scheme. Unfortunately, progress in the area of DNA-mediated self-assembly of colloids has been disappointingly slow. Recent successes at getting microcolloids^{5,6} and nanoparticles^{7,8} to crystallize have come more than a decade after the initial demonstration of the principle by Mirkin *et al.*,⁹ and DNA-mediated colloidal interactions are still not fully understood. Therefore, after outlining the principles of the proposed self-replication scheme, we will first present some results of our equilibrium and kinetics studies of the aggregation–dissociation behavior of DNA-functionalized colloids. After that, we will describe more specifically our progress on the establishment of the self-replication system.

Results and discussion

1. Colloidal self-replication: system design

An important feature of our self-replication scheme is the specificity that DNA imparts to interactions between particles coated with different sequences. Each particle species binds only to particles coated with the corresponding complementary DNA sequence and not to other particle types in the system. Moreover, as we demonstrate in Section 3, one can functionalize a particle with two or more distinct sequences, thus increasing the number of bead species it can recognize, at the same or at different temperatures. Together with the thermo-reversible nature of the

interactions, this should enable the self-replication scheme of Fig. 1a. Here, each particle species (A , A' , B and B') carries two different types of sticky ends: one facilitates permanent ‘longitudinal’ binding *inside* the replicating unit and the other provides recognition and reversible ‘transverse’ binding *between* the seed and daughter structures. The transverse sticky ends form ‘normal’ complementary pairs (A/A' and B/B'),[§] whereas the longitudinal sticky ends are self-complementary ‘palindromic’ sequences (P_1 and P_2), Fig. 1b. The longitudinal linkers are designed to form a double-stranded 5'-TA-3' stretch on either end upon hybridization. A small aromatic molecule, called psoralen, can intercalate in these TA stretches, producing a permanent cross-link when excited by long-wavelength UV radiation.¹⁰ In this way, it should be possible to permanently fix the seed and its copies. We designed all of the sequences so that they cannot hybridize with sequences that are not their intended complement. With these ingredients, our approach to obtain self-replication will be as illustrated in Fig. 1a. The initial seed, here a linear $ABABBA$ chain, is assembled at a temperature above the melting temperature of all complementary pairs in the system (for instance, using optical tweezers). Then, the temperature is lowered, so that the beads link together through hybridization of the self-complementary P_1 sequence, followed by permanent cross-linking with psoralen and UV exposure.

2. DNA-mediated colloidal interactions

2.1 The equilibrium dissociation transition. The proposed DNA-mediated colloidal self-replication scheme requires fine control over the melting temperatures of the various complementary sticky end pairs. For free DNA oligonucleotides in solution it is well-known that the melting curve depends on the sequence and number of base pairs, the DNA concentration and the ionic strength. For DNA-functionalized particles the interactions also depend on the grafting details and, in particular, the relative coverage if a bead carries multiple DNA sequences. The latter point is clearly borne out by Fig. 3a. Here, we used an equimolar mixture of beads coated with, respectively, A and A' DNA. We systematically diluted these sticky ends with ‘non-sticky’ ends, consisting of the same double-stranded backbone (Fig. 2) and a single-stranded 5'-(dT)₁₁-3' sequence, while keeping the total number of strands per bead constant at $\sim 22\,000$ (or 6400 strands/ μm^2 , from measurements using radioactively labeled DNA¹¹). For each sticky/non-sticky ratio we determined the dissociation curve, *i.e.*, the fraction of unbound particles as a function of the temperature (Fig. 3a), from a sample in a temperature gradient cell on the optical microscope (see ref. 11 for details). Clearly, the melting temperature (T_m), defined at 0.5 singlet fraction, shifts to lower values when the fraction of sticky ends becomes smaller, but the width of the dissociation transition stays nearly the same. Interestingly, if one compares these dissociation transitions with the melting curve of the same sticky ends freely suspended in solution (from optical density measurements), the transition of the beads seems to be remarkably sharp^{12,13} and it occurs at surprisingly low temperatures.

[§] Un-italicized symbols refer to the DNA sequence, italicized symbols to the particles carrying these sequences.

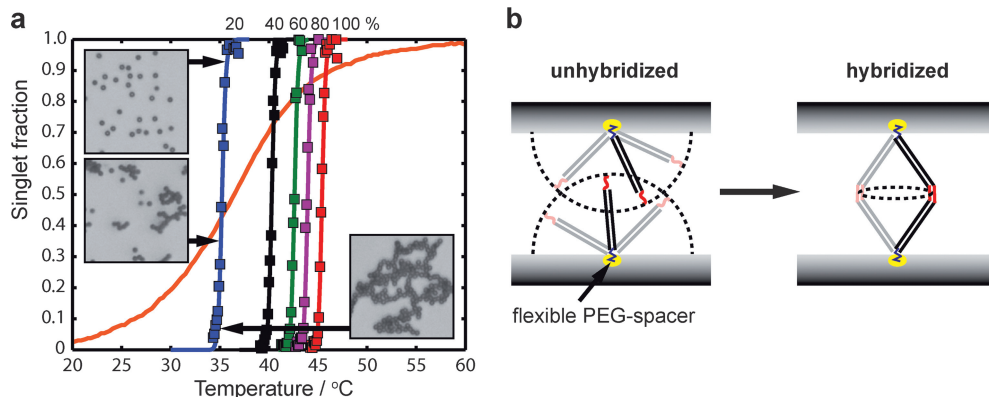


Fig. 3 The equilibrium dissociation transition as a function of the sticky end coverage. **a** The fraction of unbound beads ('singlet fraction') as a function of the temperature for equimolar mixtures of *A* and *A'* particles with a constant total DNA coverage, but a variable fraction of sticky ends, as indicated at the top of the graph. Symbols: experimental data; solid lines: fits from our theoretical model. The microscopy images show the typical appearance at different points along the dissociation transition. The broad curve in the background (solid orange line) is the melting curve of the sticky ends when freely suspended in solution (1 μ M). **b** As compared to DNA in solution, tethered DNA experiences an additional configurational entropy loss upon hybridization. Unhybridized (left), the sticky ends independently explore the surface of a half sphere, due to the flexible PEG-spacer at the 5' terminus of the DNA construct. Hybridized (right), the freedom of motion is severely restricted as the sticky ends can only move together, tracing the outline of a circle.

In ref. 11, we have developed a simple statistical mechanical model that provides a quantitative understanding of the bead dissociation transition, based on the measurable properties of the elementary constituents of the system. A direct comparison between our model and experiments revealed the crucial role played by the configurational entropy loss that is associated with the binding of tethered DNA between neighboring particles, see Fig. 3b. Thus, for a single tethered DNA bond the hybridization free energy is:

$$\Delta G_{tether} = \Delta G_{solution}^0 - T\Delta S_p$$

and for two beads that can form up to N_b bonds:

$$\Delta G_{bead} = -RT\ln(1 + ke^{-\Delta G_{tether}/RT})^{N_b}$$

Here, $\Delta G_{solution}^0 = \Delta H^0 - T\Delta S^0$ is the hybridization free energy of the sticky ends in solution, as found from optical density measurements ($\Delta H^0 = -322$ kJ/mol, $\Delta S^0 = -936$ J/molK), ΔS_p is the configurational entropy penalty (Fig. 3b), k is the number of strands on the opposing particle surface that a sticky end can choose to bind to, R is the gas constant and T is the absolute temperature. The parameters N_b and k depend on the sticky end coverage on the beads and can be estimated from geometric considerations; $N_b \approx 154$ and $k \approx 13$ for 100% coverage. Using a cell theory for the bound particles,¹⁴ together with a Flory-like aggregation model,¹⁵ we finally obtained $\Delta S_p \approx -15R$ from a fit to the experimental data. This additional entropic cost, as compared to hybridization in solution, effectively shifts the dissociation transition temperature down, enabling sharp transitions at relatively low temperatures. Importantly, we could fit all the data for different sticky end fractions with a single value for the entropic penalty (solid curves in Fig. 3a). This means that once ΔS_p is obtained from one sample of DNA-coated particles, it can subsequently be used to design the dissociation properties for other samples. Moreover, the observed sharpness of the

dissociation transition for a wide range of sticky end fractions enables a good separation of the different binding temperatures for beads with dual recognition capabilities.

2.2 The kinetics of hybridization and aggregation. To further guide our use of DNA-mediated interactions, we also studied the kinetics of the bead aggregation and dissociation for different kinds of DNA sequences and constructs. We did this by recording the particle singlet fraction (from video-microscopy³) as a function of the time, while lowering the temperature from $T > T_{m,bead}$ (52 °C) to $T \ll T_{m,bead}$ (20 °C), using different quench rates. In the second part of the experiment we gradually increased the temperature again (+3.2 °C/min). In this way, we observed dissociation transitions that were very similar in shape and width to the ones obtained in our equilibrium studies with a spatial temperature gradient, as a qualitative comparison of Fig. 3a and the up-ramps in Fig. 4 shows (around $t = 1400$ s and $t = 1300$ s in panels a and c or, equivalently, around $T = 50$ °C and $T = 45$ °C, in panels b and d respectively). During the initial aggregation process, however, we sometimes observed behavior that at first sight may seem surprising. Fig. 4a and b show the aggregation–dissociation behavior of beads coated with palindromic sticky ends that have a double-stranded backbone (Fig. 5a). This system displays the behavior one might expect for DNA-mediated colloidal interactions: once the temperature drops below the melting temperature, the singlet fraction quickly drops to zero, as the beads are incorporated into large aggregates; the quench rate only determines how fast the melting temperature is reached. If we use the same sticky ends, but now with the backbone in single-stranded form (*i.e.* without its complementary strand), we obtain aggregation–dissociation curves like the ones shown in Fig. 4c and d. These clearly depend on the quench rate in a non-trivial way: if we cool slowly (< 3 °C/min) the behavior approaches that of the double-stranded construct, but if we

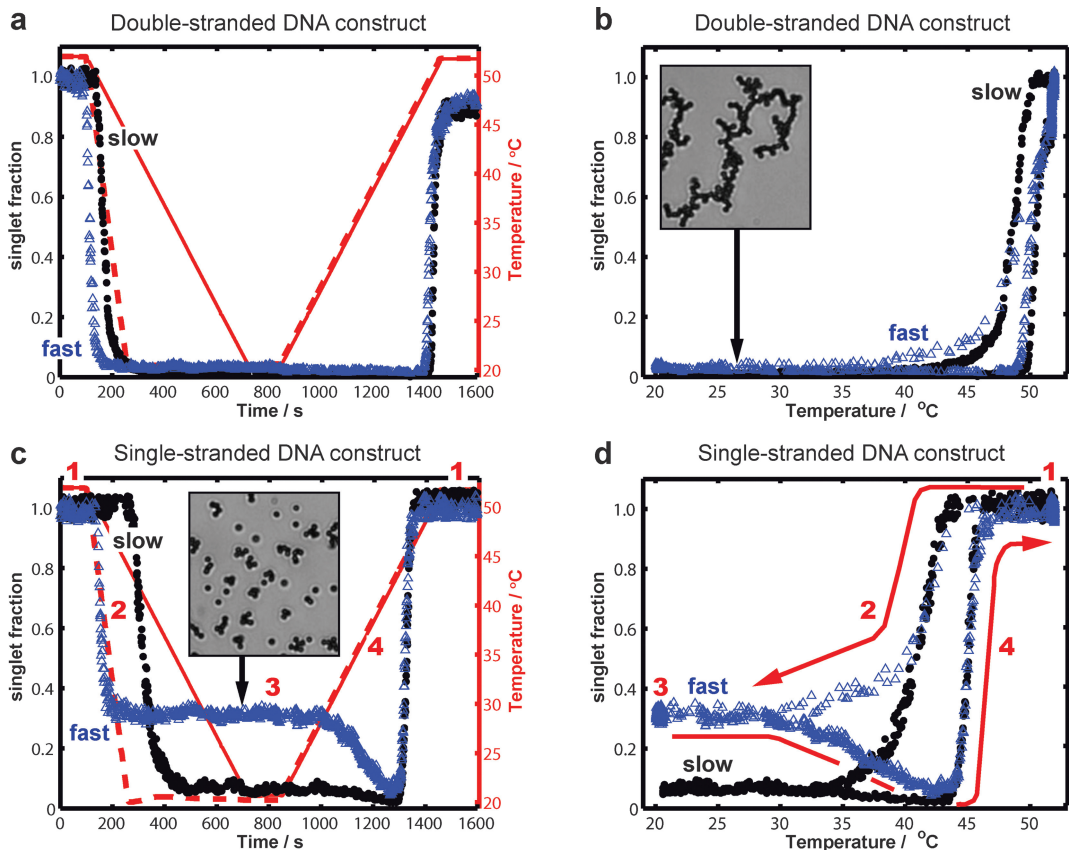


Fig. 4 Aggregation and dissociation kinetics. Temperature ramps and corresponding singlet fractions for particles functionalized with the palindromic sequence of Fig. 5a, either with a double-stranded (**a** and **b**) or a single-stranded backbone (**c** and **d**). Panels **a** and **c** on the left show the temperature (red solid and dashed lines, right axis) and the corresponding singlet fraction (dots and triangles, left axis) plotted as a function of the elapsed time, while panels **b** and **d** on the right show the same data plotted as a function of the temperature. The solid red line and black dots correspond to the slowest quench, the dashed red line and blue triangles to the fastest quench. For the fastest quench, the red arrows and indices in panels **c** and **d** indicate the relationship between the two different graphing methods. A similar relationship holds for the slow quench, as well as the data in panels **a** and **b**. Index (1) corresponds to constant high temperature, (2) to a quench from high to low temperature, (3) to constant low temperature and (4) to a ramp from low to high temperature. The insets in panels **b** and **c** are microscopy images of the samples at the end of the fastest quench (constant low temperature, '3').



Fig. 5 Intra-particle hybridization. **a** The palindromic sequence used in Fig. 4, here shown with a double-stranded backbone (in black). The sticky end is indicated in red and the bases involved in the hairpin formation of panel b-2 are underlined. **b** A schematic representation of the different forms of intra-particle hybridization that are possible with the palindromic sequence in panel a: binding between neighboring strands on the same bead for the more flexible single-stranded construct (1), hairpin formation of the sticky end with the single-stranded backbone (2), and hairpin formation of the sticky end itself, both for the single- and double-stranded constructs (3). For clarity, the particles, backbones (black) and sticky ends (red) are not drawn to scale.

quench very fast (here $12.8\text{ }^{\circ}\text{C}/\text{min}$, indicated with '2') we find that the aggregation stops at a non-zero singlet fraction, giving rise to a distinct horizontal plateau in the aggregation–dissociation curve ('3'). Moreover, when the temperature is raised again ('4'), the system first aggregates more, before the familiar dissociation transition occurs.

We can explain this remarkable behavior by a competition between different hybridization events. Here, we will only give a qualitative interpretation; the quantitative modeling will be presented in a forthcoming publication. The key ingredient is the fact that the DNA can form different bonds and secondary structures, depending on the kind of construct. Fig. 5 shows the different possibilities for the palindromic sequence that was used in Fig. 4. First of all, the single-stranded backbone (persistence length $l_p \approx 2.7\text{ nm}$)¹⁶ is much more flexible than the double-stranded construct ($l_p \approx 45\text{--}50\text{ nm}$),¹⁷ allowing these self-complementary sticky ends to bind to neighboring ones on the same bead, Fig. 5b-1. Secondly, for this particular sequence the sticky end can fold back onto the backbone and form a large hairpin, if the complementary strand of the backbone is absent, Fig. 5b-2. Finally, it is also possible for the sticky end to form a hairpin all by itself, independent of the backbone, Fig. 5b-3. In principle, each of these *intra-particle* hybridization events could compete with the formation of *inter-particle* bonds, responsible for aggregation. Which bonds dominate the system depends on the respective melting temperatures, the rates of formation and the applied quench rate. Importantly, the inter-particle binding is governed by the relatively slow diffusive time scale of the colloids, of order seconds, as compared to microseconds for the DNA hybridization time. This means that before the beads encounter each other a hybridization equilibrium will have been established within the DNA coating of each individual bead.

The peculiar aggregation–dissociation behavior of the particles with the single-stranded construct (Fig. 4c and d) can now be interpreted as follows. At the start of the quench, the particles

aggregate through the formation of multiple inter-particle bonds (from the up ramp we find $T_{m,bead} \approx 45\text{ }^{\circ}\text{C}$). However, soon after, at slightly lower temperature, the sticky ends start to bind significantly to neighboring sticky ends on the same bead (Fig. 5b-1), as these bonds have nearly the same hybridization free energy (from geometrical considerations we estimate the configurational entropy penalty for these bonds to be slightly larger, by $\sim 3R$, than the penalty for inter-particle bonds).¹¹ Neighboring sticky ends that are bound together are no longer available for inter-particle binding, leading to a sharp slowdown of the aggregation. At still lower temperature, we enter the melting curve of the hairpin structures (Fig. 5b-2/3), which have predicted^{18,19} melting temperatures of $\sim 34\text{ }^{\circ}\text{C}$. These hairpins eliminate the remaining sticky ends, causing the aggregation to stop completely. The faster the quench, the sooner the sticky ends are passivated and the less the aggregation or, in other words, the higher the plateau ('3') in Fig. 4c and d. When we raise the temperature ($t > 810\text{ s}$, '4'), the hairpins and neighbor bonds open up again, enabling more aggregation until the melting temperature of the beads is reached. In the double-stranded case, Fig. 4a and b, the binding of sticky ends to neighboring ones on the same bead is much more limited, due to the rigidity of the construct. Together with the high bead melting temperature, $T_{m,bead} \approx 50\text{ }^{\circ}\text{C}$, this means that the aggregation is complete before we reach the melting curve of the sticky-end-only hairpin (Fig. 5b-3), which is the only other structure that could significantly interfere with interparticle binding.

The experiments in Fig. 6 show that neighbor binding on the same bead can indeed cause unusual aggregation behavior, but that a complete stop of the aggregation does not occur without hairpin formation. This time, we used a different palindromic sequence with a single-stranded 'T-only' backbone, making all hairpin formation impossible. Thus, the behavior seen in Fig. 6 must be due to intra-particle bonds between neighboring sticky ends. The most important thing to notice is that the plateau in the aggregation–dissociation curve is no longer horizontal,

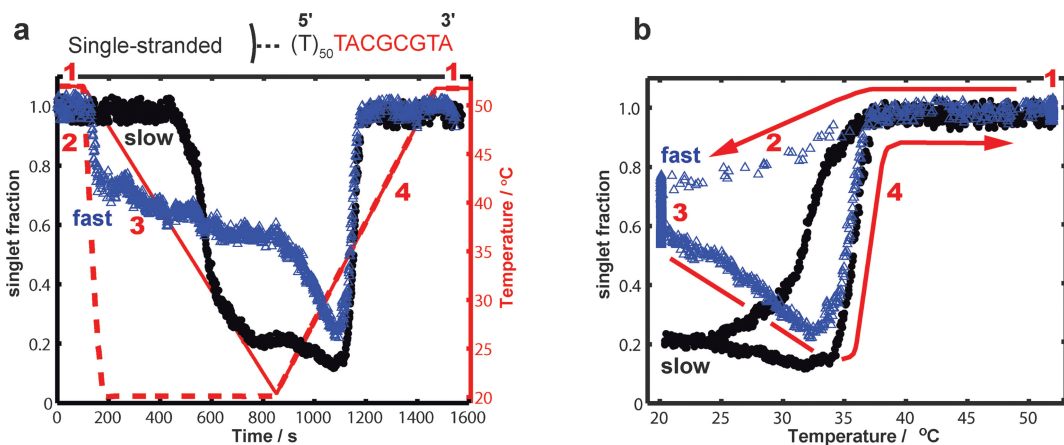


Fig. 6 The aggregation–dissociation behavior in the absence of hairpin formation. Different temperature ramps and the corresponding singlet fraction for a single-stranded palindromic sequence that does not form hairpins (sequence shown above panel **a**, with the sticky end indicated in red). Panel **a** shows the temperature (red solid and dashed lines, right axis) and the corresponding singlet fraction (dots and triangles, left axis) plotted as a function of the elapsed time, while panel **b** shows the same data plotted as a function of the temperature. The solid red line and black dots correspond to the slowest quench, the dashed red line and blue triangles to the fastest quench. For the fastest quench, the red arrows and indices indicate the relationship between the two different graphing methods; a similar relationship holds for the slow quench.

indicating that the aggregation never stops entirely. This is due to the fact that there will always be a certain fraction of sticky ends that has trouble finding a nearby partner on the same bead to bind to. The mono-molecular hairpin formation does not suffer from this ‘pairing problem’, consistent with the horizontal plateau in Fig. 4c. Taken together, Fig. 4–6 show that a rigid double-stranded construct is the safest choice for our self-replication scheme, because it nicely projects the sticky ends away from the particle surface and prevents many potential problems with unwanted forms of hybridization, especially for the palindromic sequences involved in longitudinal binding (Fig. 1b).

3. Colloidal self-replication: exploratory experiments

After the somewhat more general studies of the previous sections, Fig. 7 provides a brief overview of our current experimental progress at obtaining artificial self-replication, following the scheme presented in Fig. 1. First of all, in Fig. 7a, we demonstrate the psoralen-mediated permanent cross-linking of palindromic DNA. We find that 3 s of exposure with 365 nm UV light, using the fluorescent light source of our Leica DMRXA microscope, results in efficient cross-linking of large particle aggregates, even if we functionalize only 5% of the DNA constructs with a psoralen group. Moreover, we do not observe any adverse effects of repeated temperature cycling and UV exposure on the experimental system.

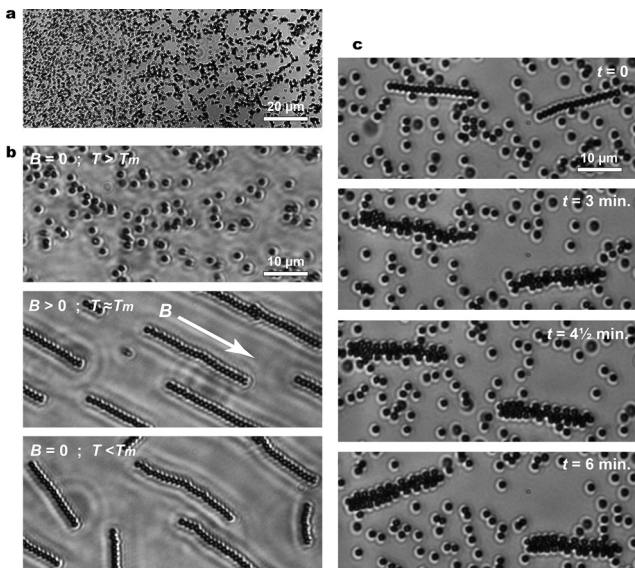


Fig. 7 Seed and daughter assembly. **a** Within 5 min at room temperature, particles coated with psoralen-functionalized palindromic DNA formed extensive aggregates. We then exposed part of the sample to UV radiation for 3 s. After heating to 45 °C, the aggregates on the left side of the microscopy image dissociated again, while the UV cross-linked structures on the right side remained intact. **b** Linear seeds were formed by applying an external magnetic field, B , while decreasing the temperature below the melting temperature (T_m) of the longitudinal palindrome bonds. The chains were then cross-linked by UV exposure. **c** Permanent ‘AAAAAA’ seeds were immersed in a bath of A' singlets and at $t = 0$ the temperature was decreased to 42 °C, which is below the transverse $A-A'$ melting temperature. Note that the sample was essentially two-dimensional, due to strong sedimentation.

In ref. 20 it was shown that DNA-coated colloids can be positioned into any desired pattern using optical tweezer arrays and we have verified that we can do the same. Eventually we will use this approach to obtain a specific order of the A and B particles, but currently we use random chain formation of magnetic polystyrene particles in an external magnetic field to quickly obtain large numbers of test seeds (Fig. 7b). After lowering the temperature below the palindrome melting temperature, the chains are kept together by longitudinal bonds. We then remove the magnetic field and form psoralen cross-links through UV exposure, resulting in rigid permanent chains. Fig. 7c and the ESI movie‡ show an experiment in which we introduced permanent ‘AAAAAA’ seeds into a bath of A' singlets (we also performed similar experiments on seeds with a random sequence of A/B particles in a bath of A'/B' singlets, giving similar results). The two bead species were covered with 80% $A/20\%$ P1 (particles A) and 80% $A'/20\%$ P2 (particles A'), giving them dual recognition capabilities. The 80/20 coverage ratio assured that the longitudinal P1 and P2 bonds had a lower melting temperature than the transverse $A-A'$ bonds (see Section 2.1), as desired for self-replication. Thus, at 42 °C the particles from the bath adhered to their complements in the seeds (from both sides) through the formation of transverse bonds, whereas longitudinal bonds only started to form when the temperature was lowered further to 39 °C (not shown). Without UV exposure, both the transverse and longitudinal bonds are fully reversible: when we increased the temperature to 45 °C the sticky ends dehybridized and the A' particles left the chain. This association-dissociation cycle could be repeated at least tens of times, while leaving the cross-linked chains intact. Moreover, association was quite fast, so that cycling of the self-replication process should be possible on a time scale of about 20 min.

In order to obtain good self-replication, we will need to pay special attention to the organization, as well as the permanent cross-linking and subsequent release of the copies. In Fig. 7c and the ESI movie,‡ one can see that the complementary particles from the surrounding bath did not only bind in the proper positions, directly on top of the seed particles, but also in the interstices between the seed particles. This may be an artifact of this particular ‘ A -only’ seed structure though, which likely can be circumvented by using an A/B or $A/B/C$ system without neighbor repeats. Due to the present imperfections in the organization, only short stretches of the daughter chains could be permanently cross-linked (through the P2 bonds). In doing so, we observed unwanted ‘cross-talk’ with the P1 sequence of the seed structure, causing poor release of the daughter chain when we raised the temperature to 45 °C or more, preventing successful copy formation. Therefore, we are currently investigating other cross-linking strategies, such as enzymatic ligation,²¹ Kool chemistry²² and the use of photo-crosslinkable polymers,²³ which could partially (e.g. only for the P2 bonds) or completely (both for P1 and P2) replace the psoralen-functionalized construct.

Conclusions and outlook

Currently, the research on nano- to microscale colloidal systems is shifting worldwide from the ‘passive’ observation of mostly equilibrium phenomena to active control over the suspension structure and self-assembly processes. With their high specificity

and thermal reversibility, DNA-mediated interactions could form a powerful tool for such directed self-assembly schemes. By studying the equilibrium and kinetic aspects of the colloidal aggregation–dissociation behavior we have acquired a better understanding of the important configurational properties of tethered DNA and, thereby, a better control over the inter-particle binding. These investigations are not only of fundamental interest, but serve a bigger goal too: the creation of a new class of materials that have sufficient information encoded in the chemical and physical properties of their building blocks both to self-assemble and to self-replicate. Here, we have presented the details of a colloidal self-replication scheme based on DNA-mediated interactions, together with the results of our first tests of its various components. This included studies of the cross-linking strategy to selectively make permanent bonds, of the dual recognition capability of bi-functionalized beads, and of the organization of bulk singlets on the seed structure.

Once we get the complete self-replication process to work, the number of copies should double every cycle. This exponential growth will greatly facilitate the fabrication of, for instance, microscopic designer components. Moreover, these easy-to-visualize colloidal systems will offer unprecedented experimental access to the mechanisms of self-organization and will provide new ways to study evolution, as the self-replication process will likely not be perfect.²⁴ While some errors will be irrelevant, other errors may propagate and compete with the original seed. From this, a primitive picture of evolution could emerge, which in turn could provide us with strategies to introduce feedback, so as to control further the processing of materials. Although we do not focus on it in our initial explorations, one could also think of ways to guide the self-assembly of the replicated building blocks into larger-scale, more complex, functional structures, as shown in Fig. 8. This can, for instance, be done with a ‘Yurke *et al.*’-type process, where certain sticky ends are protected by a complementary strand that is later removed by more favorable hybridization, thus triggering these pre-encoded interactions.^{25,26} Together with the possibility to concentrate the DNA sticky ends inside well-defined adhesive patches on the colloid surface,²⁷ this may enable highly complex, multi-step directed self-assembly/self-replication schemes.

Experimental

DNA and particle preparation

Our DNA constructs consisted of an 8–11 bases long single-stranded sticky end, at the 3' terminus of a 50 bases long ‘backbone’ oligonucleotide, which was attached to a 5' biotin group through a short, flexible polyethyleneglycol (PEG) spacer (see also Fig. 2). In so-called double-stranded constructs the backbone was hybridized from its 5' terminus to a complementary strand of 49 or, in the case of the psoralen-functionalized construct, 50 bases long. For the self-replication experiments the backbone hybridization was done at 1:1 ratio and an overall concentration of 8.5 μM (UV-260 absorption, Genequant spectrometer), for the equilibrium transition studies at 1:1 ratio and 15 μM, and for the aggregation kinetics studies at 15 μM and a 50% excess of complementary strand, all in 50 mM phosphate/50 mM NaCl hybridization buffer (pH 7.5) and by slowly cooling down from 90 to 22 °C in a water bath.

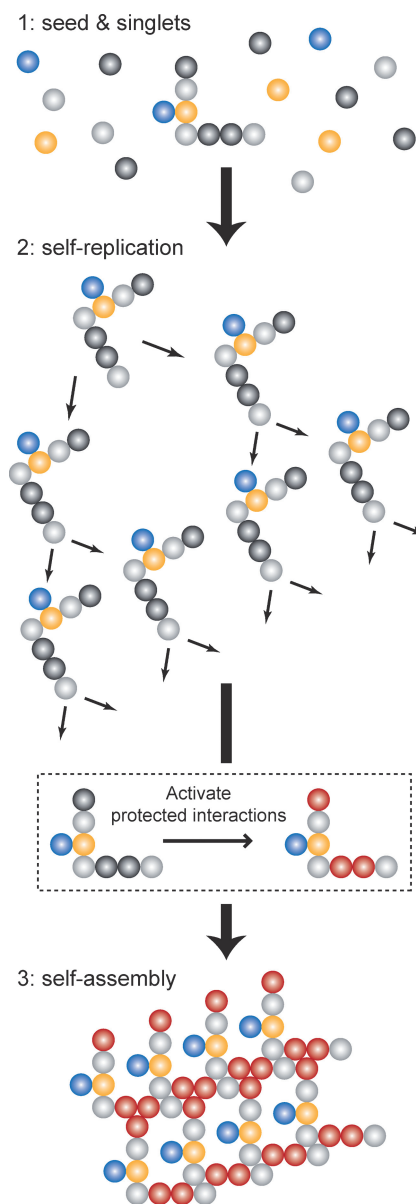


Fig. 8 Outlook: colloidal self-replication followed by triggered self-assembly. Different colloidal particles are linked together in a particular structure and this ‘seed’ is immersed in a solution of the single particles (1). The bath particles selectively interact with the particles in the seed, allowing the seed to assemble copies of itself. During this self-replication process the number of copies grows exponentially (2). At the end of the self-replication one could turn on new interactions between the particles, for instance in a Yurke *et al.*-type process (see text). These new interactions then trigger the self-assembly of the microscopic building blocks into larger-scale functional structures (3).

We obtained the oligonucleotides from Integrated DNA Technologies USA, except for some of the self-complementary palindromic sequences and the psoralen-functionalized complementary strand, which we synthesized ourselves on an Applied Biosystems 394 DNA synthesizer. After completion, we removed the oligonucleotides from the support and deprotected them using routine phosphoramidite procedures.²⁸ Psoralen was attached to the 5' terminus of the complementary strand by using Psoralen C2 Phosphoramidite (Glen Research). We designed all

of the sequences with the program SEQUIN²⁹ in order to minimize sequence symmetry.³⁰

We covered 1.05 µm diameter, streptavidin-coated polystyrene Dynabeads (MyOne Streptavidin C1, Molecular Probes) with the biotinylated DNA constructs, by incubating 5 µl bead suspension for 30 min (at room temperature or at 55 °C) with 10 µl DNA mix and 60 µl suspension buffer (10 mM phosphate/50 mM NaCl and 0.5% w/w Pluronic surfactant F127, pH 7.5) for the equilibrium studies, with 18 µl DNA mix and 52 µl suspension buffer for the self-replication experiments, and with 5 µl DNA mix and 65 µl suspension buffer for the kinetics studies. To remove excess and non-specifically adsorbed DNA we centrifuged and resuspended the particles three times in 100 µl suspension buffer; we repeated this washing procedure twice, heating in between for 30 min at 55 °C. We did not observe any signs of disintegration of the strong streptavidin-biotin bond on the time scale of our experiments.

Microscopy setup

We confined the DNA-coated particle suspensions to borosilicate glass capillaries (inner dimensions 2.0 × 0.1 mm, Vitrocom), which first underwent a plasma etching and silanization treatment. After letting the particles sediment for 5 min, we obtained an essentially two-dimensional system. For the measurement of the equilibrium dissociation transition curves we used a temperature-gradient setup on the stage of a Leica DMRXA light microscope. The setup consisted of a copper plate, of which one end was connected to a Peltier heating element (Melcor CP1.0-127-00), while the other end was cooled by a thermostatted water bath. After 1 h equilibration time, we imaged the suspension in the capillary, mounted on top of a silicon wafer, in reflection. For all of the other experiments, we glued the capillary to an ITO-coated microscopy slide with electrical contacts on either end. This slide was then placed on top of a sapphire plate on the microscope stage, which allowed for imaging in transmission mode. The ends of the sapphire plate were connected to Peltier elements, which in turn were resting on the water-cooled microscope stage, thus providing a constant background temperature. For fine temperature control we interfaced Matlab with a Lakeshore DRC 93C temperature controller, the output of which was connected with the contacts on the ITO-coated slide. The input temperature reading was provided by a platinum RTD (Pt-111, Lakeshore) attached to the top side of the ITO-coated slide.

Acknowledgements

We thank J. Bibette, I. Bischofberger, M. Clusel, J.C. Crocker, E. Eiser, D. Frenkel, O. Gang, D.G. Grier, A.J. Kim, M. Li, P.A.

Reigner, S. Sacanna, A.V. Tkachenko, M.P. Valignat, M. Weck and M. Zuker for useful discussions. This work was supported by the Keck Foundation and the Netherlands Organisation for Scientific Research (NWO).

References

- W. M. Shih, J. D. Quispe and G. F. Joyce, *Nature*, 2004, **427**, 618–621.
- J. M. Rivera, T. Martín and J. Rebek, *J. Am. Chem. Soc.*, 1998, **120**, 819–820.
- J. C. Crocker and D. Grier, *J. Colloid Interface Sci.*, 1996, **179**, 298–310.
- J. H. Holtz and S. A. Asher, *Nature*, 2003, **389**, 829–832.
- P. L. Biancaniello, A. J. Kim and J. C. Crocker, *Phys. Rev. Lett.*, 2005, **94**, 058302.
- A. J. Kim, P. L. Biancaniello and J. C. Crocker, *Langmuir*, 2006, **22**, 1991–2001.
- S. Y. Park, A. K. R. Lytton-Jean, B. Lee, S. Weigand, G. C. Schatz and C. A. Mirkin, *Nature*, 2008, **451**, 553–556.
- D. Nykypanchuk, M. M. Maye, D. van der Lelie and O. Gang, *Nature*, 2008, **451**, 549–552.
- C. A. Mirkin, R. L. Letsinger, R. C. Mucic and J. J. Storhoff, *Nature*, 1996, **382**, 607–609.
- O. Gia, S. M. Magno, A. Garbesi, F. P. Colonna and M. Palumbo, *Biochemistry*, 1992, **31**, 11818–11822.
- R. Dreyfus, M. E. Leunissen, R. Sha, A. V. Tkachenko, N. C. Seeman, D. J. Pine and P. M. Chaikin, *Phys. Rev. Lett.*, 2009, **102**, 048301.
- R. Jin, G. Wu, Z. Li, C. A. Mirkin and G. C. Schatz, *J. Am. Chem. Soc.*, 2003, **125**, 1643–1654.
- P. H. Rogers, E. Michel, C. A. Bauer, S. Vanderet, D. Hansen, B. K. Roberts, A. Calvez, J. B. Crews, K. O. Lau, A. Wood, D. J. Pine and P. V. Schwartz, *Langmuir*, 2005, **21**, 5562–5569.
- P. Charbonneau and D. Frenkel, *J. Chem. Phys.*, 2007, **126**, 196101.
- D. A. Sherman, PhD thesis, Massachusetts Institute of Technology, 1994.
- M. C. Murphy, I. Rasnik, W. Cheng, T. M. Lohman and T. Ha, *Biophys. J.*, 2004, **86**, 2530–2537.
- W. H. Taylor and P. J. Hagerman, *J. Mol. Biol.*, 1990, **212**, 363–376.
- M. Zuker, *Nucleic Acids Res.*, 2003, **31**, 3406–3415.
- Mfold server: <http://mfold.bioinfo.rpi.edu/>.
- M. P. Valignat, O. Theodoly, J. C. Crocker, W. B. Russel and P. M. Chaikin, *Proc. Natl. Acad. Sci. U. S. A.*, 2005, **102**, 4225–4229.
- S. A. Claridge, A. J. Mastroianni, Y. B. Au, H. W. Liang, C. M. Micheal, J. M. J. Fréchet and A. P. Alivisatos, *J. Am. Chem. Soc.*, 2008, **130**, 9598–9605.
- Y. Xu and E. T. Kool, *Nucleic Acids Res.*, 1999, **27**, 875–881.
- S.-J. Sung, K.-Y. Cho, H. Hah, J. Lee, H.-K. Shim and J.-K. Park, *Polymer*, 2006, **47**, 2314–2321.
- A. J. Kim, R. Scarlett, P. L. Biancaniello, T. Sinno and J. C. Crocker, *Nature Materials*, 2009, **8**, 52–55.
- B. Yurke, A. J. Turberfield, A. P. J. Mills, F. C. Simmel and J. L. Neumann, *Nature*, 2000, **406**, 605–608.
- P. Yin, H. M. T. Choi, C. R. Calvert and N. A. Pierce, *Nature*, 2008, **451**, 318–323.
- D. R. Breed, PhD thesis, University of California, 2007.
- M. H. Caruthers, *Science*, 1985, **230**, 281–285.
- N. C. Seeman, *J. Biomol. Struct. Dyn.*, 1990, **8**, 573–581.
- N. C. Seeman, *J. Theor. Biol.*, 1982, **99**, 237–247.